RAPID COMMUNICATION

Ultraviolet emissions realized in ZnO via an avalanche multiplication process*

Yu Ji(于 吉)[a)b)], Shan Chong-Xin(单崇新)[a)†], Shen He(申 赫)[a)b)], Zhang Xiang-Wei(张祥伟)[a)b)], Wang Shuang-Peng(王双鹏)[a)], and Shen De-Zhen(申德振)[a)]

[a)] *State Key Laboratory of Luminescence and Applications, Changchun Institute of Optics, Fine Mechanics and Physics, Chinese Academy of Sciences, Changchun* 130033, *China*

[b)] *University of Chinese Academy of Sciences, Beijing* 100049, *China*

(Received 26 February 2013; revised manuscript received 30 March 2013)

Au/MgO/ZnO/MgO/Au structures have been designed and constructed in this study. Under a bias voltage, a carrier avalanche multiplication will occur via an impact ionization process in the MgO layer. The generated holes will be drifted into the ZnO layer, and recombine radiatively with the electrons in the ZnO layer. Thus obvious emissions at around 387 nm coming from the near-band-edge emission of ZnO will be observed. The reported results demonstrate the ultraviolet (UV) emission realized via a carrier multiplication process, and so may provide an alternative route to efficient UV emissions by bypassing the challenging p-type doping issue of ZnO.

Keywords: avalanche multiplication, wide bandgap semiconductor, light-emitting devices

PACS: 73.40.Qv, 85.60.Jb, 73.61.Ga, 78.60.Fi **DOI:** 10.1088/1674-1056/22/7/077307

1. Introduction

Ultraviolet (UV) emissions have a variety of applications, including lighting, food sterilization, water purification, and space communication.[1,2] Wide bandgap semiconductor-based UV light-emitting devices (LEDs) have witnessed great progress in recent years.[3–9] To realize high-performance UV LEDs, the efficient generation and injection of both electrons and holes are almost indispensable. To such an end, semiconductor-based LEDs are usually realized in p–n junction structures.[10] Nevertheless, it is accepted that both the n-type and the p-type dopings of a semiconductor become more challenging as its bandgap increases, which means that it is a tough task to realize efficient UV emissions with wide bandgap semiconductors.[11,12] If carriers can be generated via a new method instead of the conventional doping route, the importance of such a method will be self-evident.

It has been reported that under a relative large electric field, the carriers in an insulator will gain much kinetic energy, the energetic carrier will impact with the lattice of the insulator to release additional carriers, and the generated carriers will again gain much kinetic energy and impact with the lattice to excite more carriers. In this way, carriers can be multiplied via the impact ionization process.[13–20]

In this paper, by employing ZnO-based wide bandgap semiconductors as an example, we show that UV emissions can be realized via the carrier multiplication caused by an impact ionization process occurring in an MgO insulation layer. The results reported here may provide an alternative promising route to efficient UV emission by bypassing the challenging p-type doping issue of ZnO.

2. Experiment

The ZnO films employed as the active layer of the UV emissions were grown on *c*-plane sapphire substrates by a sol–gel method. Zinc acetate [$Zn(CH_3COO)_2{\cdot}2H_2O$, 99.5%] was dissolved in a 2-methoxyethanol ($C_3H_8O_2$, 99.5%) and monoethanolamine (MEA, C_2H_7NO, 99.0%) solution at room temperature. Then the solution was spin-coated onto the *c*-plane sapphire substrates. The coated substrate was dried at 100 °C and then annealed in air atmosphere at 600 °C for half an hour. This cycle was repeated several times to obtain films with the desired thickness. After the growth of the ZnO film, an MgO film was deposited onto the ZnO film with a magnetron sputtering technique. Then, a thin Au layer was evaporated onto the MgO layer using a vacuum evaporation method. Interdigital electrodes were configured onto the MgO layer via a photolithography and wet etching process. The structural characterization of the ZnO films was carried out in a Bruker D8 X-ray diffractometer using Cu Kα ($\lambda = 1.54$ Å) as the excitation source. The photoluminescence (PL) spectrum of the ZnO films was recorded in a JY-630 micro-Raman spectrometer using the 325 nm line of a He–Cd laser as the excitation source. The surface morphology of the ZnO films was characterized by a Hitachi S4800 scanning electron microscope. The

*Project supported by the National Basic Research Program of China (Grant No. 2011CB302005), the National Natural Science Foundation of China (Grant Nos. 11074248, 11104265, 11134009, and 61177040), and the Science and Technology Developing Project of Jilin Province, China (Grant No. 20111801).

†Corresponding author. E-mail: shancx@ciomp.ac.cn

© 2013 Chinese Physical Society and IOP Publishing Ltd

electrical characteristics of the films and the devices were measured using a Lakeshore 7707 Hall measurement system, and electroluminescence (EL) measurements were carried out in a Hitachi F4500 spectrometer with a continuous current power source. Note that all the measurements were performed at room temperature.

3. Results and discussion

In the Hall measurement, the ZnO film shows n-type conduction with an electron concentration of 2.7×10^{16} cm^{-3} and a Hall mobility of 0.4 cm$^2\cdot$V$^{-1}\cdot$s^{-1}. The surface morphology of the ZnO film is displayed in the inset of Fig. 1(a), from which a film with a rough surface can be observed, and many hillocks as indicated by the white spots can be seen. The room temperature PL spectrum of the ZnO film is shown in Fig. 1(a), and the spectrum shows a strong emission at around 377 nm, which is the typical near-band-edge emission of ZnO, while the defect-related emission centered at around 500 nm is weak. The X-ray diffraction (XRD) pattern of the ZnO film is shown in Fig. 1(b). All the peaks are associated with ZnO, indicating that the ZnO film is polycrystalline without any preferred orientations.

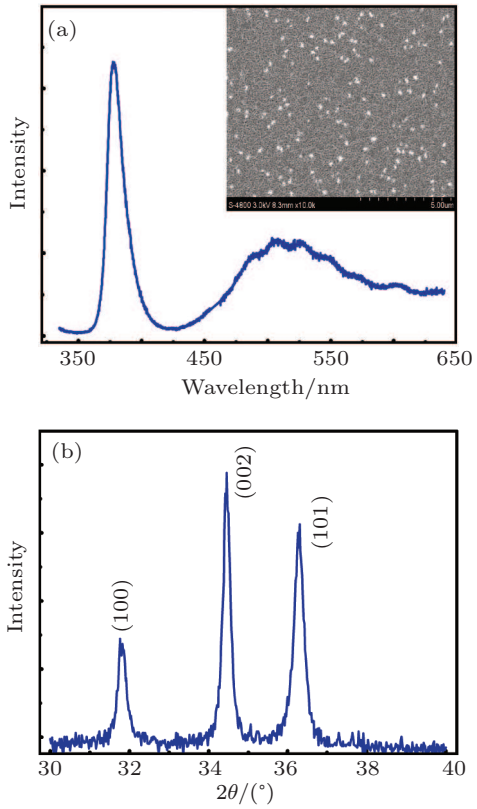


Fig. 1. (color online) (a) The PL spectrum of the ZnO film, with the inset showing the surface morphology of the ZnO film; (b) the XRD pattern of the ZnO film.

To realize carrier multiplication, an Au/MgO/ZnO/MgO/Au structure was designed and constructed; and a schematic illustration of the structure is shown in the inset of Fig. 2. The thickness of the ZnO film is about 180 nm, and that of the MgO layer is about 60 nm. The interdigital Au fingers are 500 μm in length and 5 μm in width, and the inter-electrode spacing is 5 μm. The current–voltage (I–V) characteristic of the device under dark conditions is illustrated in Fig. 2. The current of the device increases gradually as the applied bias increases, and it tends to saturate when the bias is 12 V. A noteworthy phenomenon is that the current shows a further rapid increase when the bias voltage is over 52 V, which is an indication of carrier avalanche multiplication.[21,22] The above facts reveal that a carrier multiplication has occurred when the bias voltage is larger than 52 V.

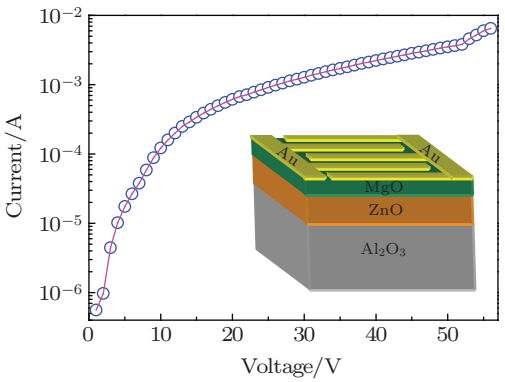


Fig. 2. (color online) The I–V characteristics of the Au/MgO/ZnO/MgO/Au structure, with the inset showing a schematic diagram.

To further understand the carrier multiplication process, a bandgap diagram of the Au/MgO/ZnO/MgO/Au structure biased at 52 V is shown in Fig. 3(a). The Au/MgO/ZnO/MgO/Au structure has two Schottky barriers connected back-to-back. A bias of any polarity will put one Schottky barrier in the reverse direction and the other in the forward direction. As the applied voltage increases, the barrier height for holes lying in the forward bias contact is lowered and the hole current increases, so the current increases initially with the increasing bias voltage. When the applied voltage is larger than the flat-band voltage, most of the voltage will drop on the MgO layer lying in the reverse bias contact due to the dielectric nature of the MgO layer, and the electric field in a certain area may be in the order of 10^6 V/cm. Under such a strong electric field, holes that enter into the MgO layer will be greatly accelerated. The accelerated holes may impact with the lattice of the MgO layer to release their kinetic energy and create additional electrons and holes. The generated electrons and holes will again gain much kinetic energy from the strong electric field and create more electrons and holes. In this way, carrier multiplication occurs and the current increases rapidly via the impact ionization process.[23]

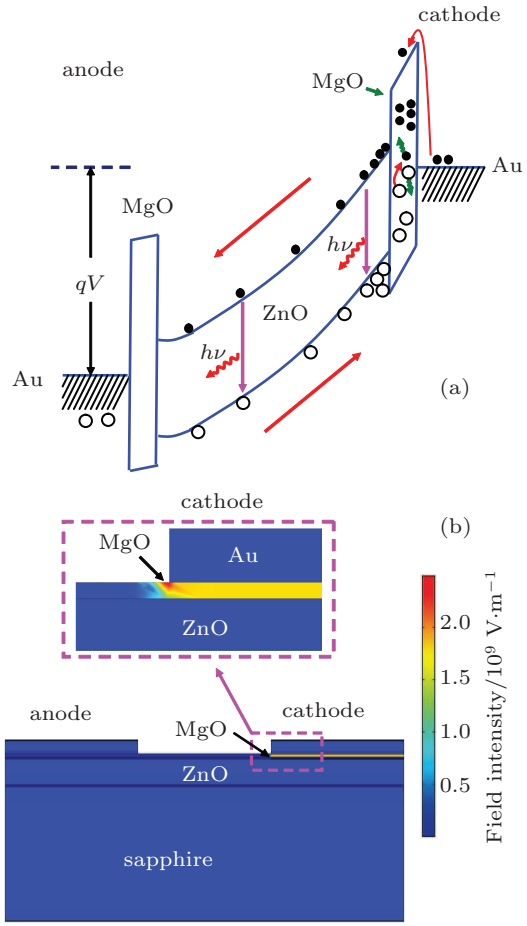


Fig. 3. (color online) (a) The bandgap diagram of the Au/MgO/ZnO/MgO/Au structure under a bias voltage, and (b) the electric field distribution in the structure at 52 V.

To verify the above analysis, the two-dimensional (2D) electric field distribution in the Au/MgO/ZnO/MgO/Au structure is calculated by using COMSOL Multiphysics, as shown in Fig. 3(b). One can see from the figure that the electric field in the MgO layer underneath the cathode is the strongest, and impact ionization tends to occur firstly in localized regions along the cathode contact edge. The corresponding critical electrical field in the multiplication region is about 25 MV/cm, which is above the reported critical impact ionization threshold in MgO.[15]

Once the electrons and holes generated in the impact ionization process recombine in the ZnO layer, UV emissions may be realized. To this end, the emission of the Au/MgO/ZnO/MgO/Au structure under bias voltages is measured, and the emission spectra of the structure are shown in Fig. 4. One can see that obvious emissions can be detected from the structure, and two emission bands can be distinguished. The one at around 387 nm comes from the near-band-edge emission, while the one at around 550 nm is the deep-level emission of ZnO. The UV emission is enhanced even more remarkably with respect to the defect-related emissions with the increase of the bias voltage. The dependence of the integrated emission intensity of the structure on the bias voltage applied is shown in the inset of Fig. 4. Initially, the emission intensity increases slowly with the increasing bias voltage, however, it increases abruptly when the bias voltage is over 52 V. We note that this value accords well with the threshold voltage for the carrier avalanche multiplication, which consolidates that the emission is closely related to the carrier multiplication process.

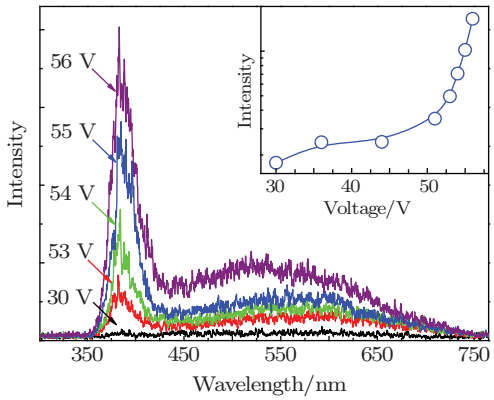


Fig. 4. (color online) Room-temperature emission spectra of the Au/MgO/ZnO/MgO/Au structure under different biases. The inset shows the dependence of the integrated emission intensity of the structure on the bias voltage.

4. Conclusion

In conclusion, UV emissions were realized in Au/MgO/ZnO/MgO/Au structures, and the emissions were found to come from the radiative recombination of the holes generated via an impact ionization process occurring in the MgO layer under a relatively large electric field and the electrons in ZnO. We note that the UV emissions obtained by the avalanche multiplication process have not been reported before, and thus the results reported in this paper may provide a promising alternative route to efficient UV emissions by bypassing the challenging p-type doping issue of ZnO, and may be applicable to other wide bandgap semiconductors.

References

[1] Khan A, Balakrishnan K and Katona T 2008 *Nat. Photon.* **2** 77
[2] Simon J, Protasenko V, Lian C, Xing H and Jena D 2010 *Science* **327** 60
[3] Ambacher O 1998 *J. Phys. D: Appl. Phys.* **31** 2653
[4] Jiao S J, Zhang Z Z, Lu Y M, Shen D Z, Yao B, Zhang J Y, Li B H, Zhao D X, Fan X W and Tang Z K 2006 *Appl. Phys. Lett.* **88** 031911
[5] Yan Q R, Yan Q A, Shi P P, Niu Q L, Li S T and Zhang Y 2013 *Chin. Phys. B* **22** 026102
[6] Zhang S, Wang X P, Wang L J, Zhu Y Z, Mei C Y, Liu X X, Li H H and Gu Y Z 2010 *Chin. Phys. B* **19** 097805
[7] Feng Q J, Jiang J Y, Tang K, Lu J Y, Liu Y, Li R, Guo H Y, Xu K, Song Z and Li M K 2013 *Acta Phys. Sin.* **62** 057802 (in Chinese)
[8] Yan Q R, Zhang Y, Yan Q A, Shi P P, Zheng S W, Niu Q L, Li S T and Fan G H 2012 *Acta Phys. Sin.* **61** 036103 (in Chinese)
[9] Wang F F, Cao L, Liu R B, Pan A L and Zou B S 2007 *Chin. Phys.* **16** 1790

[10] Zhu H, Shan C X, Li B H, Zhang Z Z, Yao B and Shen D Z 2011 *Appl. Phys. Lett.* **99** 101110
[11] Look D C, Claflin B, Alivov Y I and Park S J 2004 *Phys. Stat. Sol. A* **201** 2203
[12] Ni P N, Shan C X, Wang S P, Li B H, Zhang Z Z and Shen D Z 2012 *Opt. Lett.* **37** 1568
[13] Ma X Y, Chen P L, Li D S, Zhang Y Y and Yang D R 2007 *Appl. Phys. Lett.* **91** 251109
[14] Chen P L, Ma X Y and Yang D R 2006 *Appl. Phys. Lett.* **89** 111112
[15] Zhu H, Shan C X, Zhang J Y, Zhang Z Z, Li B H, Zhao D X, Yao B, Shen D Z, Fan X W, Tang Z K, Hou X H and Choy K L 2010 *Adv. Mater.* **22** 1877
[16] Chen P L, Ma X Y, Li D S, Zhang Y Y and Yang D R 2007 *Appl. Phys. Lett.* **90** 251115
[17] Yu J, Shan C X, Qiao Q, Xie X H, Zhang Z Z, Wang S P and Shen D Z 2012 *Sensors* **12** 1280
[18] Cheng J B, Zhang B, Duan B X and Li Z J 2008 *Chin. Phys. Lett.* **25** 262
[19] Ren H X and Hao Y 2001 *Chin. Phys.* **10** 189
[20] Xu X B, Zhang H M, Hu H Y, Li Y C and Qu J T 2011 *Chin. Phys. B* **20** 108502
[21] Xie F, Lu H, Chen D J, Xiu X Q, Zhao H, Zhang R and Zheng Y D 2011 *IEEE Electron Dev. Lett.* **32** 1260
[22] McClintock R, Yasan A, Minder K, Kung P and Razeghi M 2005 *Appl. Phys. Lett.* **87** 241123
[23] Sze S M, Coleman D J and Loya A 1971 *Solid-State Electron* **14** 1209